International Journal of Fluid Power 4 (2003) No. 3 pp. 17-25

NUMERICAL OPTIMIZATION OF A DISTRIBUTOR VALVE

Leon Dahlén[1) and Peter Carlsson[2)

1)Department of Engineering, Physics and Mathematics, Mid-Sweden University, 831 25 Östersund, Sweden
Leon.Dahlen@mh.se
2)Department of Information Technology and Media, Mid-Sweden University, 831 25 Östersund, Sweden
Peter.Carlsson@mh.se

Abstract

In this paper a non-linear optimization method is used to improve the design of a distributor valve. The distributor valve is an important component in a radial piston hydraulic motor, and optimization of the design to minimize power losses is an interesting way to increase efficiency. The main function of a distributor valve is to supply the pistons with a pressurized flow and to return oil during rotation. At the same time the distributor valve acts as an externally pressurized lubricated thrust bearing, in order to separate the rotating parts from the motor case. The bearing acts as a hydrostatic annular multi-recess plane thrust bearing, with different recess pressures. The separating force of the bearing is balanced hydrostatically by the pressure that is applied and springs. Losses will occur in the contact between the parts in the distributor valve, due to friction and leakage.

This paper shows that modern optimization methods can be used as an effective tool to create new designs and to modify the existing design of the bearing surface geometry of the distributor. A finite element method has been used to simulate the contact, and the program is linked to an optimization routine to perform the optimization. The results of the optimized design show a significant decrease in power loss, compared to the existing design in the operating range.

Keywords: radial piston hydraulic motor, simulations, optimization, power loss

1 Introduction

Hydraulic pumps and motors are expected to work under a wide range of operating conditions, and finding the optimum design of components can be difficult. When optimizing a hydraulic machine for maximum efficiency, an accurate model of the physical behaviour governing flow and torque losses is needed. Coefficient models derived from the physical behaviour of the losses provide a helpful tool for a qualitative understanding of the phenomena governing losses in hydraulic machines. However, for optimization purposes it is necessary to go one step further and investigate the individual sources of losses in the component.

In most cases experimental tests are performed to compare and evaluate the properties of different design solutions, which take time and are costly. A cost saving method, in time and money, is to evaluate different solutions using computer-aided simulations. By combining simulation with an optimization method, a significant reduction of time in the developing process can be achieved.

This manuscript was received on 14 April 2003 and was accepted after revision for publication on 06 October 2003

In this paper a sliding contact in a radial piston hydraulic motor is studied. The hydraulic motor is of cam-lobe design and a cross-section of the motor is shown in Fig. 1.

The motor has an even number of pistons that operate in sequences of working pressure and charge pressure in a reciprocating motion. The casing is stationary, which means that the cylinder block and piston assembly rotate. The pistons are operated via a cam roller in contact with the curved track cam ring, which is fixed to the motor casing. In the motor mode, the piston assembly moves radially outwards under working pressure and inwards during idling.

The hydraulic motor is often used as the driving unit in industrial hydrostatic transmissions, which are used in a number of different applications, such as shredders, crushers, conveyors, mixers and cement kilns. Often the transmissions run almost continuously and, as their power consumption can be high (in the order of MW), energy efficiency has become an important issue. Sealing and bearing gaps are one of the essential design elements of displacement machines. The gaps usually undertake two different functions: as sliding bearings between parts that move in relation to one other, and to accomplish a sealing function (Ivantysynova, 1999).

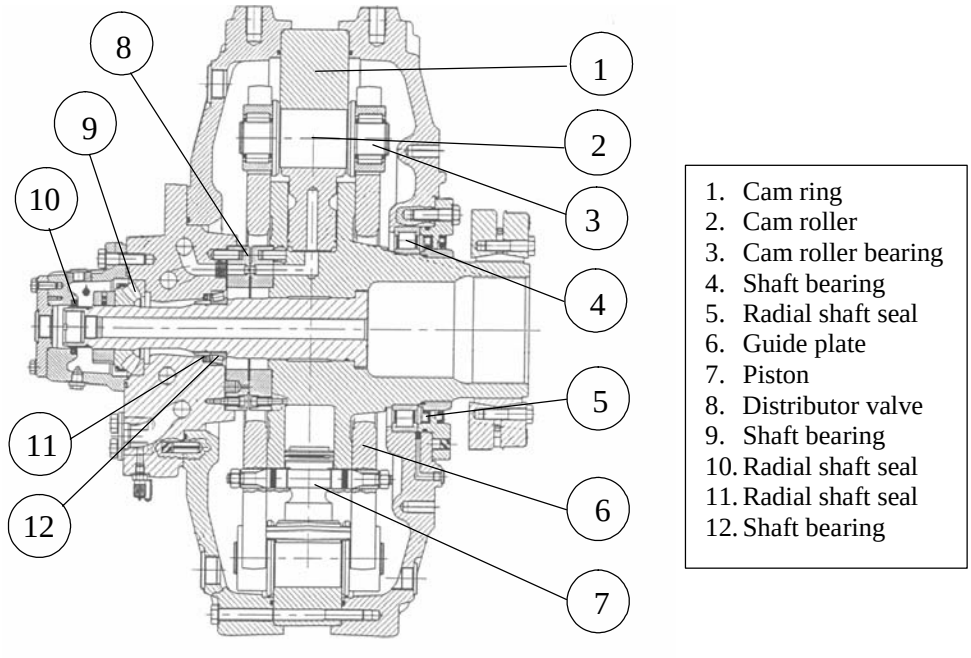

Fig. 1: *Cross-section of the hydraulic motor*

The efficiency and durability of hydraulic equipment is clearly influenced by the tribological characteristics of the bearing/sealing parts that have been investigated by different authors, e.g. Ludema (2001) and Yamaguchi (1997).

In a radial piston motor the distributor valve (8) acts, in additions to other functions, as a multi-recess hydrostatic plane thrust bearing. Externally pressurized bearings are commonly used in hydraulic units and have been investigated by several authors, e.g. O'Donoghue and Rowe (1970) and Koc and Sahlin (2000). The losses in hydrostatic machines are influenced to a large extent by the friction and leakage flow in the different lubricating gaps within the machine (Ivantysynova, 1999). To aid the computation of gap flow, several different simulation models have been presented, e.g. Zhu et al (1992), Fang and Shirikashi (1995), Kleist (1997) and Wieczorek and Ivantysynova (2002). In a previous paper by the authors of this paper Dahlén and Olsson (2002) two sliding contacts inside the radial piston hydraulic motor were studied, one of which was the distributor valve. The aim of the previous study was to investigate the torque losses in these contacts and also to discover if and when a change in lubrication regime could be expected in these contacts.

In the present study the distributor valve is studied and an optimization of the bearing geometry of the contact between the plates of the distributor valve is performed. The optimization of hydraulic systems or hydraulic units has been carried out by several researchers using different methods of optimization in order to find an optimal solution. Some of these methods have an analytical approach Rowe et al (1970), Younes (1993) and Kazama and Yamaguchi (1993), while others use numerical methods, e.g. Rydberg (1983), Xy and Chen (1998) without consideration of the changes in the properties of the fluid under running condition.

In this study a numerical method is used to optimize the geometry of the contact in the distributor valve, taking changes in the properties of the fluid due to running conditions into account. The contact between the plates in the distributor valve has been simulated as a hydrostatic annular multi-recess plane bearing, and the geometry of the bearing surface has been optimized with regard to power losses. The simulations have been carried out using a FEM software package, available on the commercial market (Solvia, 1999) and have been linked to an optimization routine MMA (method of moving asymptotes) (Svanberg, 1993) to perform the optimization. The FEM software makes it possible to study the fluid film behaviour between loaded sliding surfaces, taking fluid properties into account, such as viscosity-temperature-pressure inter-dependency, heat conduction and heat convection.

2 The Simulation of a Distributor Valve

The distributor valve distributes oil to the piston bores. The valve consists of two plates, as shown in Fig. 2, one distributor fixed to the connection block and one port plate that moves with the cylinder block.

To control the separation between the surfaces, the plates are pressed together by balancing pistons and balancing sleeves, in addition to springs, under normal operating conditions. Simulation of power loss in the distributor valve have been made using the FEM software package, supposing that full film lubrication is the probable lubricating regime. A description of the software package operation mode is presented in Appendix A. The interacting surfaces between the two plates have been modelled as a hydrostatic annular multi-recess plane bearing, with different recess pressures, which works against a plane surface. In Fig. 3 the internal geometry of the distributor of the model is shown. In

order to simplify the model, the geometry of the recess pads differs somewhat from the actual geometry in the distributor, which has rounded corners and smooth opening phases on the mean diameter.

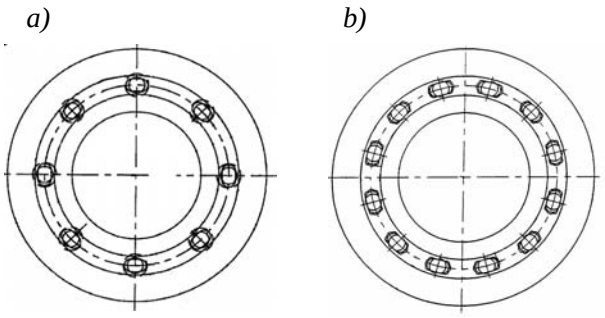

Fig. 2: *Schematic drawing of the port plate (a) and the distributor (b)*

However, the area of the bearing load carrying surface has remained unaltered. The distributor is assumed to be rigid in the model and does not conduct any heat.

In the optimization process, a 60° element of the distributor is used, which is illustrated in Fig. 3. The 60° element has been modelled in the same way as the full model of the distributor. By using a 60° element in the optimization process, the time of each iteration will be reduced significantly without affecting the results in a decisive way. The results of the optimization have been used to simulate the power loss of the full model of the distributor. In both models a mesh grid of 8-node elements has been used to construct the fluid film. The number of node elements in the full model in the circumferential direction is 90 and in the radial direction 6. The pressure boundary conditions of the film surface are specified, so that the pressure at the outer and inner radius of the annular multi-recess bearing is equal to zero. The twelve recess pads are alternately pressurized by low and high pressure. To perform the simulations the relevant recess pressure, motor speed, film thickness, bearing geometry nad fluid properties are needed as input data. The high pressure is in the range of 5 MPa to 30 MPa and the low pressure is set to 1.5 MPa during the simulations, which correspond to the operating range of the motor. A maximum motor speed of 30 rpm down to 0.5 rpm and a film thickness from 3 µm up to 12 µm have been used in the simulations. The simplified design of the distributor has a bearing of the following dimensions: inner radius (R_i) 77.5 mm, outer radius (R_y) 93.5 mm, pad inner radius (r_i) 79.5 mm, pad outer radius (r_y) 91.5 mm and recess-pad angle (φ_p) 13.76°. The thickness of the plate is 35 mm. The physical properties of the fluid, such as the viscosity temperature – pressure dependency, density, heat conduction and heat convection were based on a synthetic polyalphaolefin ISO VG 100 and are shown in Table 1. The temperature of the fluid flow to the high-pressurized pads was 40 °C, to the low-pressurized pads 45 °C and in the reservoir 40 °C, in order to simulate real conditions from an experimental test done by Dahlén and Olsson (2002). In Fig. 4 the boundary conditions for the bearing are shown.

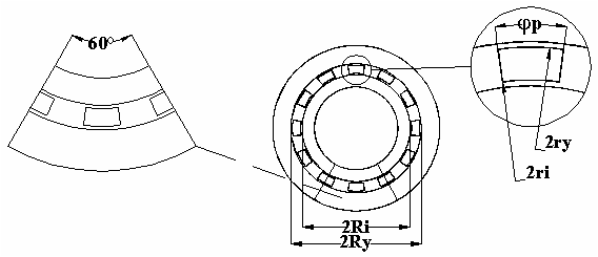

Fig. 3: *Simplified geometrical model of the distributor and the 60° element*

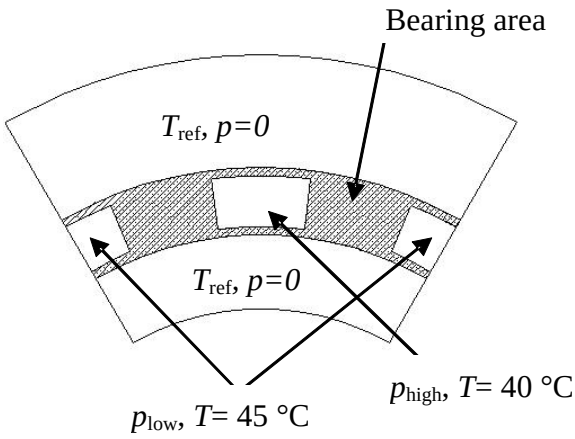

Fig. 4: *Bearing boundary conditions*

Table 1: Physical data for the synthetic fluid ISO VG 100

Viscosity at 40 °C μ (Pa s)	$97.3 \cdot 10^{-3}$	
Density at 40 °C ρ (kg/m^3)	852	
Pressure-viscosity coefficient α (m^3/N)	$1.8 \cdot 10^{-8}$	
Temperature-viscosity coefficient β (1/°C)	0.036	
Conductivity k (W/(m °C))	10 °C 0.145	150 °C 0.159
Specific heat c (J/(m^3 °C))	10 °C $1.81 \cdot 10^6$	150 °C $2.23 \cdot 10^6$

3 Optimization

In order to improve the efficiency of the hydraulic motor, optimization is used to change the design of the bearing surface of the distributor valve. Generally the mathematical discipline optimization or programming, as it often is called, is used to minimize (or maximize) an objective function $f(\boldsymbol{x})$, often with certain restrictions or constraints $g_i(\boldsymbol{x})$. Compared with traditional design, the optimization process can be described as a sort of reverse design process: instead of calculating the quality of a given design, optimization starts with the desired performance characteristics and, based on that, calculates a design which fulfils the demands. Optimization is an iterative process in which it is usual that a

convex sub-problem is generated and solved in each iteration. The solution of the sub-problem gives a new design point, which should be closer to the optimum, and the process usually converges to reach a local optimum. A schematic description of the process is shown in Fig. 5. In this paper, the MMA-method is used as an optimization routine (MMA, Method of Moving Asymptotes) Svanberg (1987 and 1993). MMA is based on the values of the objective function and the constraints functions and on their derivatives, in relation to the design variables at the design point. It has been used with great success in a variety of examples including structural optimization, fluid-flow, wood drying and acoustic optimization, e.g. Esping et al (1993), Carlsson and Esping (1997) and Tinnsten et al (1999).

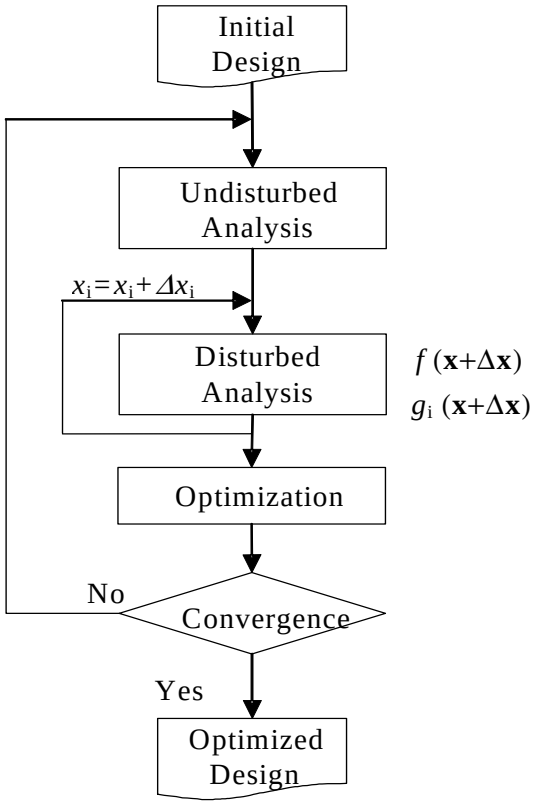

Fig. 5: *Data flow chart during optimization*

In this application, the purpose of the optimization is to minimize the film power loss in the distributor valve (the objective function) at the same time as the area of the recess-pad is the same as in the original design. The reason to keep the recess-pad area constant is to minimize the effect on flow characteristic through the valve. Design variables are the inner radius r_i and the outer radius r_y and the angle of the recess-pad φ_p, see Fig. 3. In mathematical terms, the optimization problem can be formulated as follows:

Minimize

$$f(\boldsymbol{x}) \equiv P \tag{1}$$

so that

$$g_1(\boldsymbol{x}) \equiv A_p = A_p^{\text{original}} \tag{2}$$

where $P = P(\boldsymbol{x})$ is the power loss in the distributor valve.

$A_p = A_p(\boldsymbol{x}) = \pi \frac{\varphi_p}{360}\left(r_y^2 - r_i^2\right)$ is the area of the recess-pad.

A_p^{original} is the original area of the recess-pad.

$\boldsymbol{x} = (r_i, r_y, \varphi_p)$ is the vector of the design variables.

Since MMA only allows inequality constraints, the area constraint is divided into two constraints as shown below:

$$g_1(\boldsymbol{x}) \equiv (1-\varepsilon)A_p \le A_p^{\text{original}} \tag{3}$$

$$g_2(\boldsymbol{x}) \equiv A_p^{\text{original}} \le (1+\varepsilon)A_p \tag{4}$$

where ε is a small number.

Since there are no explicit expressions of the film power loss, the necessary derivatives must be calculated as numerical approximations. In this case finite differences are used for the derivative calculations, and, for example, the derivative of the film power loss (P) with respect to the inner radius r_i is calculated as:

$$\frac{\partial P}{\partial r_i} \approx \frac{P(r_i + \delta r_i) - P(r_i)}{\delta r_i} \tag{5}$$

where δr_i is the perturbation of r_i. To calculate $P(r_i)$, a complete calculation is performed with the undisturbed values of the variables. For the next calculation, the inner radius r_i is perturbated by δr_i, and this gives a new value of $P = P(r_i + \delta r_i)$ and it is now possible to calculate the ratio of Eq. 5. In order to calculate all the derivatives, all variables must be perturbated in this way, see Fig. 5. With help of the inner loop around the disturbed analysis, and the undisturbed analysis above the loop, necessary derivatives and function values are calculated. All the values are passed through the optimization routine, which calculates a new proposal for the design variables $\boldsymbol{x}$. If the optimization process has converged, the calculation is complete, otherwise the calculation continues with more iterations in the outer loop. The variables $\boldsymbol{x}$ are permitted to vary within the range shown below:

r_i; [0.077; 0.085] m
r_y; [0.085; 0.093] m
φ_p; [10°; 16°]

At start the variables have the values of the simplified geometry: φ_p = 13.76°; r_i = 0.0795 m; r_y= 0.0915 m. The original recess-pad area is $A_p^{\text{original}} = 246.4 \cdot 10^{-6}$ m^2. The width of the lands between the recess-pad and the inner radius R_i and outer radius R_y of the contact in the distributor valve are equal in the original geometry. The power loss, leakage, maximum temperature and bearing force of the simplified and optimized geometry have been simulated in the full model of the distributor.

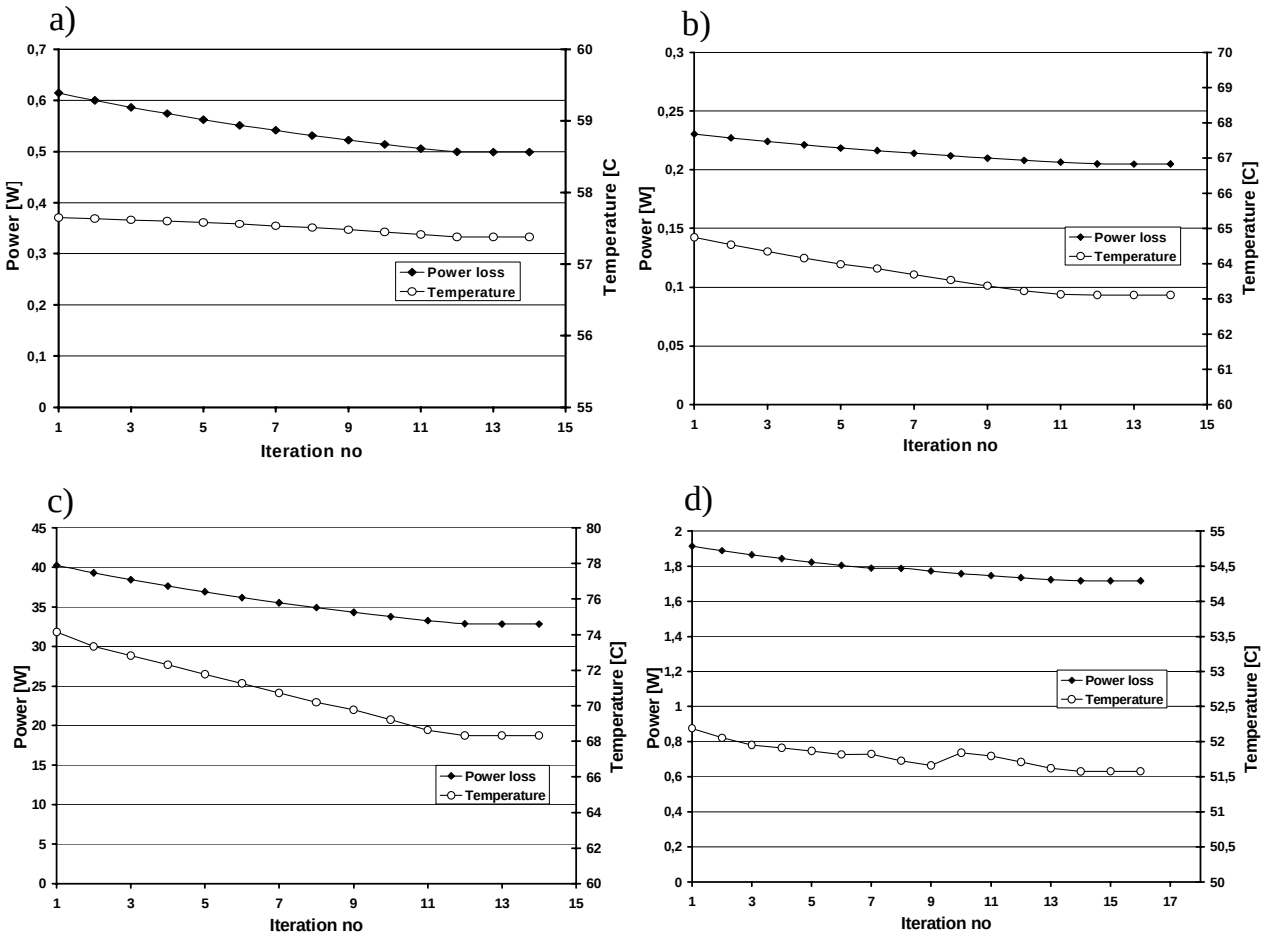

Fig. 6: *Results from optimization of the 60° element under different operating conditions of recess - pressure, motor speed and film thickness*
a). Recess-pressure 30 MPa, motor speed 0.052 rad/s and film thickness of 3 μm
b). Recess-pressure 15 MPa, motor speed 1.047 rad/s and film thickness of 3 μm
c). Recess-pressure 30 MPa, motor speed 3.142 rad/s and film thickness of 12 μm
d). Recess-pressure 5 MPa, motor speed 3.142 rad/s and film thickness of 12 μm

4 Results

The results of the optimization of the geometry with regard to power loss in the distributor are presented for four different operating conditions or starting points in the optimization process. The operating conditions, pressure to the high pressure pads, motor speed and film thickness varied in the optimization process as follows:

- High pressure and low speed
- Medium pressure and medium speed
- High pressure and high speed
- Low pressure and high speed

The film thickness was 3 μm in the first two cases and 12 μm in the last two cases. Figure 6 illustrates the history of the objective function, i.e. the power loss together with the maximum temperature in the contact when optimizing the 60° element under different operating conditions.

In all cases the power loss decrease and an observable decrease of the maximum temperature can be noticed in the optimized geometry. In Fig. 7 the history of the optimized geometry in the case of high pressure, low motor speed and a film thickness of 3 μm is shown, and is similar in all cases. The differences in operating conditions, such as recess-pressure, motor speed or film thickness, do not affect the result in the optimization of the geometry. The object function, i.e. the power loss in 60° element, converges after 12 iterations as shown in Fig. 6. Figure 7 shows that the angle φ increases to the maximum value, while the inner and outer radii do not reach their limits.

In Table 2 the numerical values of the design variables for the original and the optimized geometries are shown. The results show that the outer land at the recess-pads will increase more compared to the inner land in order to minimize the power loss. The pad angle φ_p has increased from the starting point of 13.76° to the maximum value of 16° in the optimized geometry.

Table 3: Results from simulation of full model of the simplified and optimized design of the distributor under different operating conditions

Operating Conditions	Simulating Properties	Simplified Distributor	Optimized Distributor	Difference
p_p = 30 MPa Ω = 0.0524 rad/s h = 3 µm	Power loss [W]	3.9	3.0	-22.5 %
	Max temperature [°C]	57.6	57.4	-0.2 °C
	Leakage [m^3/s]	$1.35 \cdot 10^{-7}$	$1.05 \cdot 10^{-7}$	-22.6 %
	Bearing force [N]	$7.71 \cdot 10^{4}$	$7.64 \cdot 10^{4}$	-0,9 %
p_p = 15 MPa Ω = 0.524 rad/s h = 3 µm	Power loss [W]	1.4	1.2	-14.3 %
	Max temperature [°C]	64.3	63.1	-1.2 °C
	Leakage [m^3/s]	$6.91 \cdot 10^{-8}$	$5.41 \cdot 10^{-8}$	-21.8 %
	Bearing force [N]	$4.15 \cdot 10^{4}$	$4.12 \cdot 10^{4}$	-0.5 %
p_p = 30 MPa Ω = 3.142 rad/s h = 12 µm	Power loss [W]	252.8	197.0	-22.1 %
	Max temperature [°C]	71.6	68.3	-3.3 °C
	Leakage [m^3/s]	$8.71 \cdot 10^{-6}$	$6.74 \cdot 10^{-6}$	-22.6 %
	Bearing force [N]	$7.71 \cdot 10^{4}$	$7.63 \cdot 10^{4}$	-1.0 %
p_p = 5 MPa Ω = 3.142 rad/s h = 12 µm	Power loss [W]	11.8	10.2	-13.3 %
	Max temperature [°C]	53.1	52.5	-0.6 °C
	Leakage [m^3/s]	$1.77 \cdot 10^{-6}$	$1.38 \cdot 10^{-6}$	-22.2 %
	Bearing force [N]	$1.69 \cdot 10^{4}$	$1.69 \cdot 10^{4}$	0 %

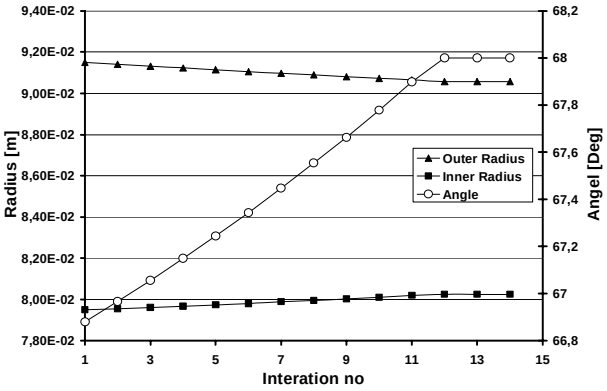

Fig. 7: *History of the design variables*

In Table 3 the results of simulations of the full model of the original and optimized geometries of the distributor are presented for different operating conditions. The bearing force is the separating force created by the pressure distribution between the plates of the distributor valve, and has to be balanced in this application. The leakage is the total leakage in the distributor valve. Table 3 also presents the maximum temperature reached in the contact of the distributor valve.

Table 2: Simplified and optimized geometries of the recess-pad in the distributor valve

Variables	Simplified Geometry	Optimized Geometry
Inner radius r_i [mm]	79.50	80.25
Outer radius r_y [mm]	91.50	90.57
Pad angle φ_p [degree]	13.76°	16.00°
Inner land (r_i-R_i) [mm]	2.00	2.75
Outer land (R_y-r_y) [mm]	2.00	2.93

5 Discussion

The size of the bearing surface in the distributor has not been changed i.e. the inner radius (R_i) and the outer radius (R_y) are constant during optimization; only the geometry of the recess-pads has been changed. The area of the recess-pad has also been constant during the optimization in order to minimize disturbances of flow characteristic of the valve. By making small changes of the geometry and the position of the recess-pad area in the distributor a significant reduction of power loss has been achieved. Optimization of the geometry of the distributor is independent of starting point e.g. operating conditions in the operating range.

The optimized geometry shows a decrease of power loss in the distributor up to 22% under certain operating conditions. Under all the operating conditions tested a decrease of power loss between 13 – 22% was obtained. The reduction of power loss is greater as a percentage at higher pressure, and is not affected in any significant way by the motor speed or film thickness in the operating range.

In the optimized geometry the leakage was reduced by 22% in the operating range, which indicates that the leakage seems to be the main reason for the power loss. If this is the case the optimization will increase the length of the clearances in order to minimize the leakage. In all the cases tested the maximum temperature in the contact was constant or decreased in the optimized distributor.

In the original geometry the outer and inner land of the recess-pad was equal. In the optimized geometry the outer land became greater compared to the inner in order to minimize the power loss. In this case the outer land increased from 2 mm to 2.93 mm (46.5%) and the inner from 2 mm to 2.75 mm (37.5%). At the same time the pad angle increased to the maximum value. It

is obvious that if leakage is the main reason for the power loss, the length of the clearance will increase in the optimization process. The optimization routine optimizes the distribution of the size of the clearance length between the inner and outer land, in order to minimize the power loss.

The bearing capacity, i.e. the bearing force, will not change significantly. Only 1 % or less reduction of the bearing force in the optimized geometry has been noted. This means that a small change in the balancing force will achieve the same compressing force in the distributor valve.

The change in power loss due to the second function of the distributor valve, i.e. as a flow channel to the piston bore, has not been considered in this study. The film thickness has been assumed to be constant during simulation and optimization. In real the pressure and temperature distribution will create elastic and thermal deformation on the distributor valve and thereby might influence the film thickness. Conducted heat into solids of the distributor has not been considered in this work.

6 Conclusion

This method of using simulation software linked to an optimization routine offers the possibility of optimizing complex, multi-variable, non-linear problems. An analytical solution can be hard to find when there are many constraints involved. Numerical optimization offers a method where many constraints can be applied to the problem and an optimal solution can be found.

From the results and discussion, the following conclusions can be drawn:

- A simulation package linked to an optimization algorithm can be used successfully to optimize the design of a distributor valve, taking changes in the properties of the fluid under different operating conditions into account.
- Through small changes in the recess-pad geometry a significant reduction of power loss in the distributor has been achieved.
- The main part of the power loss comes from the leakage in the distributor.
- The optimized geometry of the distributor does not affect the bearing capacity significantly.
- The optimized geometry is not affected by the operating conditions.

Nomenclature

A_p	recess-pad area	[m^3]
P	power loss	[W]
R_y	distributor outer radius	[m^2]
R_i	distributor inner radius	[m^2]
T	temperature	[°C]
c	specific heat	[J/(m^3 °C)]
g_i	constraint, i = 1,2	
h	film thickness	[m^2]
k	conductivity	[W/(m °C)]
p	pressure	[Pa]
r_y	pad outer radius	[m^2]
r_i	pad inner radius	[m^2]
$u_{a,b}$	velocity	[m/s]
$v_{a,b}$	velocity	[m/s]
x_j	design variable, i	
$\boldsymbol{x}$	vector of design variables	
Φ	heat source	[W]
α	pressure-viscosity factor	[m^3/N]
φ_p	recess-pad angle	[°]
μ	viscosity	[Pa s]
ρ	density	[kg/m^3]
τ	shear stress	[N/m^2]

References

Carlsson, P. and **Esping, B.** 1997. Optimization of the wood drying process. *Structural Optimization*, Vol. 14, pp. 232-241.

Dahlén, L. and **Olsson, H.** 2002. Analysis of two sliding contacts inside a radial piston hydraulic motor. *5th JFPS International Symposium on Fluid Power*, Nara, Japan.

Esping, B., Holm, D. and **Romell, O.** 1993. The OASIS-ALADDIN structural optimization system. *Int. Ser. Num. Math.*, Vol. 110, pp. 159-186.

Fang, Y. and **Shirakashi, M.** 1995. Mixed Lubrication Characteristics Between the Piston and Cylinder in Hydraulic Piston Pump-Motor. *Transactions of the ASME*, Vol. 117.

Ivantysynova, M. 1999. A New Approach to the Design of Sealing and Bearing Gaps of Displacement Machines. *Fourth JHPS International Symposium*, Tokyo, Japan.

Ivantysynova, M. 1999. Ways for Efficiency Improvements of Modern Displacement Machines. *Sixth Scandinavian International Conference on Fluid Power (SICFP '99)*, Tampere, Finland.

Kazama, T. and **Yamaguci, A.** 1993. Optimum design of bearing and seal parts for hydraulic equipment. *Wear*, Vol. 161 (1993), pp. 161-171.

Kleist, A. 1997. Design of Hydrostatic Bearing and Sealing Gaps in Hydraulic Machines. *5th Scandinavian International Conference on Fluid Power*, Linköping, Sweden.

Koc, E., and **Sahin, B.** 2000. A theoretical investigation into the design and performance of hydrostatic bearings. *Modelling, Measurement and Control B*, Vol. 69, No. 5-6, ISSN: 1259-5969, pp. 19-34.

Ludema, K. C. 2001. Tribological design: A real world approach, Hydraulic failure analysis: Fluids, Components and System effects. *ASTM STP 1339, G. E. Totten, D. K. Wills and D. G. Feldmann, Eds., American Society for Testing and Materials*, West Conshohocken, PA.

O'Donoghue, J. P. and **Rowe, W. B.** 1970. Design of multi-recess hydrostatic bearings. *Machinery and*

production engineering, 14 October 1970, pp. 622-626.

Rowe, W. B., O´Donoghue, J. P. and **Cameron, A.** 1970. Optimization of externally pressurized bearings for minimum power and low temperature rise. *Tribology*, Vol. 3, No. 3, pp. 153-157.

Rydberg, K-E. 1983. *On performance optimization and digital control of hydrostatic drives for vehicle applications*. Linköping Studies in Science and Technology, Dissertation No. 99, Linköping, Sweden.

SOLVIA system 99.0, SOLVIA Engineering AB, Sweden, 1999.

Svanberg, K. 1987. MMA – Method of moving asymptotes – A new method for structural optimization. *Int. Journal Num. Meth. Eng.*, Vol. 24, pp. 359-373.

Svanberg, K. 1993. The method of moving asymptotes (MMA) with some extensions. *Rozvany, G.I.N. (ed) Optimization of large structural optimization, (Proc. NATO/DFG ASI, held in Berchtesgarden, Germany, 1991)*, Dordrecht: Kluwer, pp. 555-578.

Tinnsten, M., Esping, B. and **Jonsson, M.** 1999. Optimization of acoustic response. *Structural Optimization*, Vol. 18, pp. 36-47.

Wieczorek, U. and **Ivantysynova, M.** 2002. Computer aided optimization of bearing and sealing gaps in hydrostatic machines - the simulation tool CASPAR. *International Journal of Fluid Power*, Vol. 3, No. 1, pp. 7-20.

Xu, S. and **Chen, B.** 1998. Optimum design and automatic drawing of recessed hydrostatic bearings. *Proceedings of the Leeds-Lyon symposium on tribology*, Paper XIV(i), pp. 411-418.

Yamaguchi, A. 1997. Tribology of hydraulic pumps. *ASTM Special Technical Publication*, No. 1310, pp. 49-61. (Proceedings of the 1995 Symposium on Tribology of Hydraulic Pump Testing, Dec 4-5 1995, Houston, TX, USA, pp. 49-61).

Younes, Y. K. 1993. A revised design of circular bearings for optimal pumping power. *Tribology international*, Vol. 26, No 3, pp. 195-200.

Zhu, D., Cheng, H. S., Arai, T. and **Hamai, K.** 1992. A Numerical Analysis for Piston Skirt in Mixed Lubrication - Part I and II. *Journal of Tribology*, Vol. 114, pp. 553-562, Vol. 115, pp. 125-133.

Appendix

Software package

A simulation of the sliding contact is achieved using the FEM software package Solvia (1999). The software makes it possible to consider the fluid film behaviour between loaded sliding surfaces, taking the properties of fluids into account, such as viscosity-temperature-pressure inter-dependence, heat conduction and heat convection. The pressure distribution in the film is given by the Reynolds Eq. 6.

$$\frac{\partial}{\partial x}\left(\frac{\partial p}{\partial x}\frac{h^3}{12\mu}\right)+\frac{\partial}{\partial y}\left(\frac{\partial p}{\partial y}\frac{h^3}{12\mu}\right)=\frac{\partial}{\partial x}\left(h\,\tilde{u}\right)+\frac{\partial}{\partial y}\left(h\,\tilde{v}\right) \tag{6}$$

where

$$\tilde{u}=\frac{u_a+u_b}{2} \qquad \tilde{v}=\frac{v_a+v_b}{2}$$

Due to the gap flow of a viscous fluid, the fluid and the contact surfaces are heated up by the dissipated energy. Hence the energy Eq. 7 is solved simultaneously in the model:

$$\rho\, c\,\frac{DT}{Dt}=div\left(k\cdot gradT\right)+\Phi \tag{7}$$

The term on the left side of the equation represents the heat convection. The first term on the right side describes the heat conduction and the second term the viscous dissipation function. Assuming a Cartesian system of coordinates, the energy dissipation Φ can be written as:

$$\Phi=\tau_x\frac{\partial u}{\partial z}+\tau_y\frac{\partial v}{\partial z} \tag{8}$$

In each temperature interval [T_i, T_{i+1}], the local change of dynamic fluid viscosity due to temperature and pressure is considered in the model to be:

$$\mu=\mu_i\, e^{K(T-T_i)}\cdot e^{[\alpha_i+L(T-T_i)]p} \tag{9}$$

$$K=\frac{\ln\mu_{i+1}-\ln\mu_i}{T_{i+1}-T_i} \tag{10}$$

$$L=\frac{\alpha_{i+1}-\alpha_i}{T_{i+1}-T_i} \tag{11}$$

where

μ_i is absolute fluid viscosity at temperature T_i.

μ_{i+1} is absolute fluid viscosity at temperature T_{i+1}.

α_i is pressure factor at temperature T_i.

α_{i+1} is pressure factor at temperature T_{i+1}.

A two-dimensional film element is used to represent the fluid film between the sliding surfaces. The fluid film is generated by film elements of 8, 16 or 18 nodes shown in Fig. 8. The film elements are used in stationary analyses, where the fluid film pressure is calculated. The fluid temperature may either be specified by the user or can be calculated by the program. The film elements are non-linear and full Newton equilibrium iterations are performed. The film elements are formulated by an interpolation of the fluid film mid-surface

pressures and temperatures, using the prevailing film thickness. Each iteration step consists of calculations of the increments in pressure, temperature and displacement. The applied force/moment tolerances govern the convergence, since a small change in pressure or temperature usually means a relatively large change in force/torque.

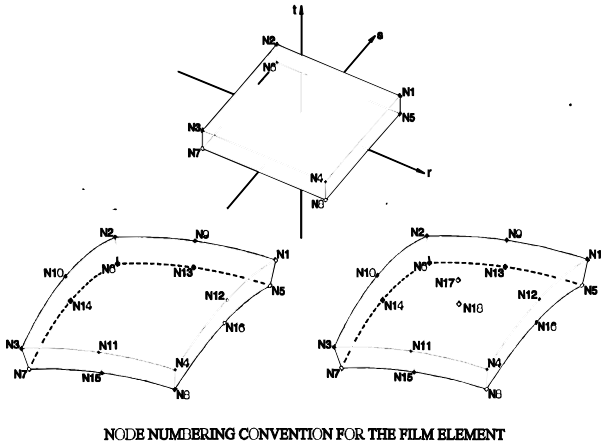

Fig. 8: *The 8, 16 and 18 node elements*

Based on the surface velocity specified for the film top surface, the pressure boundary conditions, the film thickness and the fluid viscosity, a discrete form of Reynolds Eq. 6 is used to calculate the pressure distribution. The pressure distribution and the specified surface velocity determine the volume flow of the oil film and the shear stresses that act on the sliding surfaces. The fluid temperature distribution in the film thickness direction is averaged at a fictitious mid-surface node based on the temperature at the top and at the bottom of the film element.

The mid-surface temperatures are determined from the discretization of the fluid film energy Eq. 7. The shear stresses in the fluid film cause heat to be generated. The volume of the fluid flow calculated together with the pressure causes a convective transport of heat. The boundary conditions for the convective heat flow are defined by specifying the temperature distribution at the fluid film inlet.

The inlet node temperature is taken from the reservoir node, which has to be specified in the model. The film element can transport heat by conduction in the transverse direction of the film, driven by the temperature difference between the top and bottom surface nodes and the fictitious mid-surface nodes. Heat conduction from the top and bottom of the film element can be transported further by conduction via the element surface nodes. In Fig. 9 the calculation flow chart is shown, using the pressure applied or load as input data. The outputs from the simulations, when the convergence criteria are reached, are pressure, flow and temperature distribution, reaction force/torque, displacement, minimum film thickness, leakage and power loss in the contact.

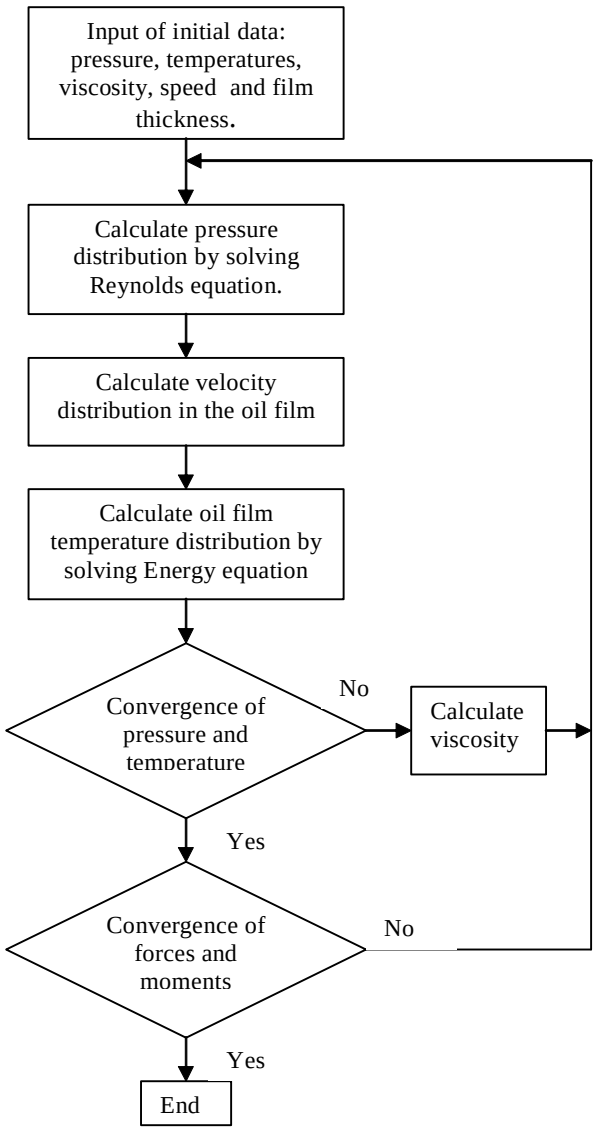

Fig. 9: *Data flow chart during simulations*

Leon Dahlén
Born on December 28th 1950 in Hoting (Sweden). Study of Mechanical Engineering and M.Sc. at Luleå University of Technology, Luleå, Sweden. Ph.D. at the Division of Machine Element, Luleå University of Technology, Luleå, Sweden with a Doctoral Thesis on Numerical and Experimental Study of Performance of a Hydraulic Motor. Assistant master at Mid Sweden University, Östersund, Sweden.

Peter Carlsson
Born on April 14th 1950 in Östersund (Sweden). Study of Mechanical Engineering and M.Sc. at Chalmers University of Technology, Göteborg, Sweden. Ph.D. at Royal Institute of Technology, Stockholm, Sweden with a Doctoral Thesis on Optimized Wood Drying. Assistant professor at Mid-Sweden University, Östersund, Sweden.